Growth of Platinum Clusters via Addition of Pt(II) Complexes: A First Principles Investigation

Lucio Colombi Ciacchi* and Wolfgang Pompe

Institut für Werkstoffwissenschaft, Technische Universität Dresden, D-01069 Dresden, Germany

Alessandro De Vita

Dipartimento di Ingegneria dei Materiali e Chimica Applicata, Università di Trieste, I-34100 Trieste, Italy, and INFM-DEMOCRITOS National Simulation Center, Trieste, Italy

Received: August 6, 2002; In Final Form: December 2, 2002

The growth of platinum clusters by the addition of Pt(II) complexes to clusters with an average oxidation state higher than zero is investigated by means of first principles molecular dynamics. In the simulations, $PtCl_2(H_2O)_2$ complexes react with Pt_{12}, $Pt_{12}Cl_4$, and $Pt_{13}Cl_6$ clusters with no need for reducing electrons. The analysis of the electronic density of states of the growing clusters shows that immediately after the adsorption of the Pt(II) complex on the cluster surface the electronic states of the complex extend over the whole cluster. In a process that gradually increases the mean coordination number of the atoms within the cluster, the adsorbed Pt atom is progressively incorporated into the cluster structure and quickly becomes indistinguishable from the other Pt atoms. Considerable rearrangement of the cluster structure and redistribution of the chlorine ligands on the cluster surface characterize the observed reactions. These results are fully consistent with the autoaccelerating kinetics observed in cluster growth experiments and support a face-capping growth mechanism that can account for shape-controlled cluster fabrication.

I. Introduction

The mechanisms through which metal clusters and colloids form in solution have received a great deal of attention in recent years.[1−5] This is due to the importance of achieving an accurate control of the nucleation and growth processes, which is necessary to produce clusters of uniform size[6,7] and shape.[8] Monodisperse colloidal suspensions present optimal catalytic properties[9] and can be employed for the production of self-assembled particle arrays with peculiar electronic and optical properties.[10−12] Moreover, the controlled, selectively heterogeneous metal growth on biomolecular templates allows for the fabrication of nanosized metal structures in a perfectly clean surrounding medium.[13] To improve the control of all phases of the cluster-formation process, a detailed understanding of the elementary steps of cluster growth is desirable.

In this work, we study the mechanism of metal cluster growth on the atomic scale by means of molecular dynamics techniques taken to the quantum accuracy level.[14,15] Our goal is to obtain a detailed picture of the agglomeration reactions that take place during the reduction of a metal salt solution and eventually lead to colloid formation. The initial nucleation of platinum clusters after the reduction of hydrolyzed $PtCl_4^{2-}$ ions was studied in a previous investigation.[1] We found that the addition of one electron to a $PtCl_2(H_2O)_2$ complex leads to the formation of a linear $PtCl_2^-$ complex after the detachment of both water ligands. Unexpectedly, in a series of dynamical simulations, we then observed that a platinum dimer can form in solution at this stage of the reduction process through the reaction of an unreduced $PtCl_2(H_2O)_2$ complex with a singly reduced $PtCl_2^-$ complex. The Pt−Pt bond forms via electron donation from the d_{z^2} orbital of the Pt(II) complex to the half-filled HOMO orbital of the Pt(I) complex.[1] This led to the hypothesis that analogous reactions may happen on the surface of open-shell clusters (not necessarily completely reduced to the zero-valent state) and may be an important process for the overall mechanism of growth. Here we perform direct simulations of the addition reaction of $PtCl_2(H_2O)_2$ complexes to growing clusters in various reduction states.

The development of metal clusters in solution proceeds primarily via an autocatalytic surface-growth mechanism in which metal ions are adsorbed on the cluster surface and reduced in situ.[3,5] The presence of Pt(II) ions adsorbed on the surface of colloids has been claimed after a spectroscopic investigation.[16] In the case of radiolytic reduction processes, radicals are expected to transfer electrons to the nucleated particles so that metal complexes are reduced on the particle surface by the accumulated electrons.[17] More generally, the formation of zero-valent atoms in solution, which later aggregate to form a cluster, is not thermodynamically favored and can be ruled out for platinum[2] and other noble metals.[17−19] Instead, the reduction of ions on the surface of clusters, in competition with the capping action of the stabilizer, can account for shape-specific growth under a controlled reduction rate and stabilizer concentration.[4] In general, the size and shape distribution of colloidal particles can be controlled by tuning the ratio between the stabilizer and the metal concentration in the solution.[8,20,21] In the case of rhodium−carbonyl clusters, the electrophilic addition of Rh(I) complexes to the square faces of octahedral ligated Rh_{13} clusters leads to Rh_{14} and Rh_{15} clusters,[22] suggesting a simple growth pathway. Other growth processes, for example,

* Corresponding author. Present address: Theory of Condensed Matter Group, Cavendish Laboratory, University of Cambridge, Madingley Road, Cambridge CB3 0HE, U.K. E-mail: lc316@cam.ac.uk. Fax: +44 (0)1223 337356.

10.1021/jp026698f CCC: $25.00
Published on Web 02/04/2003

the agglomeration of small particles,[23] can be avoided by carefully tuning the reaction conditions.[7]

Despite extensive investigations on the cluster-growth process, little is known about the interactions between metal complexes and clusters in solution.[3,9,16] An atomistic model of the addition reactions responsible for the growth of clusters is not yet available. Theoretical considerations about possible patterns for cluster growth have been made on the basis of static calculations with structure optimization at various precision levels, taking into account naked clusters.[24−29] However, to our knowledge, no dynamical simulation of the aggregation of complexed metal atoms to ligated metal clusters has been carried out so far. In this work, we perform first principles simulations of the adsorption of complexed Pt(II) ions to growing Pt clusters. In this study, we do not attempt to model the electron-transfer processes between a reducing agent and the clusters or the complexes. Our simulated systems contain from the beginning the number of electrons necessary for the desired global oxidation state. (See ref 1.)

II. Computational Details

All first principles molecular dynamics simulations[14] are performed using the Car−Parrinello (CP) method[15] within the framework of the spin-polarized density functional theory (DFT).[30] We use the gradient-corrected exchange-correlation potential PW91[31] and separable, norm-conserving atomic pseudopotentials.[32] The wave functions and the electron density are expanded on a plane-wave basis set up to kinetic energy cutoffs of 50 and 200 Ry, respectively. Periodic boundary conditions are used, considering only the valence Bloch electrons at the Γ point of the Brillouin zone. Given the metallic character of small noble-metal clusters,[33,34] our CP simulations are performed with the algorithm proposed in refs 35 and 36 to treat metallic systems. In the dynamical calculations, the electronic states are occupied according to a Fermi distribution with a smearing temperature T_S corresponding to $k_B T_S = 0.25$ eV. This value is lowered to $k_B T_S = 0.05$ eV for a more precise determination of the Fermi energy in the static calculations.[37] For the Pt atom, we use the scalar-relativistic pseudopotential with 18 valence electrons described in ref 1. This yields a lattice constant of 3.98 Å and a bulk modulus of 233 GPa for crystalline platinum.[38] These values compare well with the results of a recent DFT calculation[39] (3.98 Å and 237 GPa, respectively) and with the experimental values of 3.92 Å and 278 GPa.[40] In the FPMD simulations, the mass of the hydrogen atoms is increased to 4.0 amu, the fictitious electronic mass in the CP method is set to 300 au, and a time step of 6.0 au (about 0.145 fs) is used. All calculations have been carried out on the massively parallel CRAY-SGI computer platforms of the Center for High Performance Computing at the Dresden University of Technology using the LAUTREC code.[41]

III. Results

We present here the results of simulations in which we model the addition of Pt complexes to Pt_{12} clusters. With this choice of cluster size, the addition reaction leads to a Pt_{13} cluster, which is the first atomic closed-shell structure according to the series of Chini magic numbers.[42−44]

A. Naked Pt_{13} Cluster. Our investigation begins with the study of the naked cluster Pt_{13} in the cubooctahedral and icosahedral geometries (Figure 1, top). In spin-unrestricted calculations, we find that after full atomic relaxation the clusters present in both cases an open electronic shell with a total spin of $S = 3$. The icosahedral geometry is found to be more stable

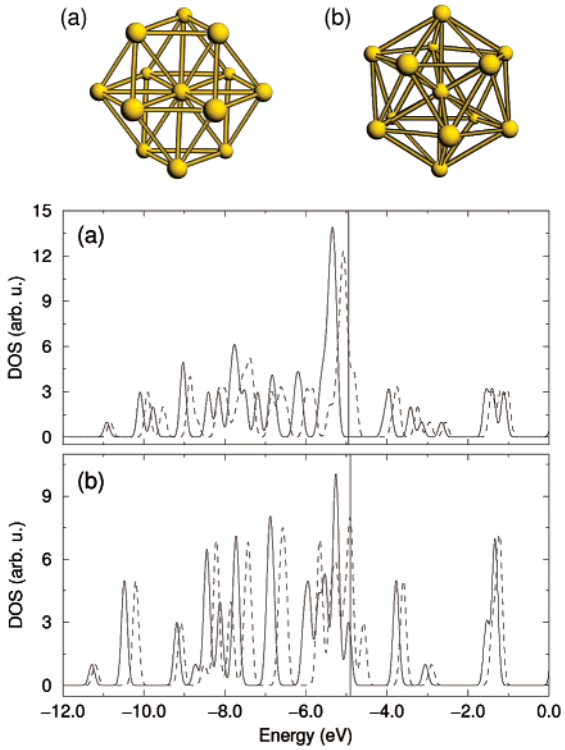

Figure 1. Top: cubooctahedral (a) and icosahedral (b) naked Pt_{13} clusters. Bottom: plot of the density of states near the Fermi level (indicated by a vertical line) for the cubooctahedral (a) and the icosahedral (b) Pt_{13} clusters. (—) Spin-majority component. (- -) spin-minority component.

than the cubooctahedral geometry by 0.57 eV.[45] At equilibrium, the Pt−Pt distance between the central atom and the peripheral atoms is 2.72 Å in the cubooctahedral cluster and 2.67 Å in the icosahedral cluster. A plot of the density of state (DOS) near the Fermi level is shown for both cluster structures in Figure 1 (bottom). The two spin manifolds appear to be occupied according to the "big atom" model.[46−48] Namely, the d electronic shell is completely filled in the majority spin manifold and is partially unfilled in the minority spin manifold. For the cubooctahedral cluster, the calculated HOMO−LUMO energy gaps associated with the electronic spectra of the majority and minority spin manifolds are 1.18 and 0.08 eV, respectively. For the icosahedral cluster, the energy gaps are 1.17 and 0.04 eV, respectively.

B. Naked Pt_{12} Cluster. To find a Pt_{12} structure corresponding to a local minimum of the potential energy surface, we start from a configuration of 12 Pt(0) atoms arbitrarily arranged in a BCC structure, with Pt−Pt neighbor distances of about 3.3 Å. The system is first annealed for ∼2 ps in a constant-temperature FPMD simulation at 600 K, and then the atomic motion is slowly quenched until the equilibrium geometry of Figure 2 is reached. The final structure consists of a central Pt atom surrounded by the other 11 atoms. The presence of three 2-fold symmetry axes and one 3-fold symmetry axis in the cluster structure is illustrated in Figure 2. The 32 Pt−Pt bonds present in the cluster have a mean Pt−Pt distance of 2.73 Å.

In the ground state, the electronic structure of the Pt_{12} cluster presents a total spin of $S = 2$. The HOMO−LUMO energy gaps are 0.41 and 0.05 eV for the majority and minority spin manifolds, respectively. We also computed the electronic structure of the Pt_{12} cluster by imposing the constraint of zero spin (spin-paired calculation). In this case, the total energy of the cluster is 0.22 eV higher than in the ground state, and the

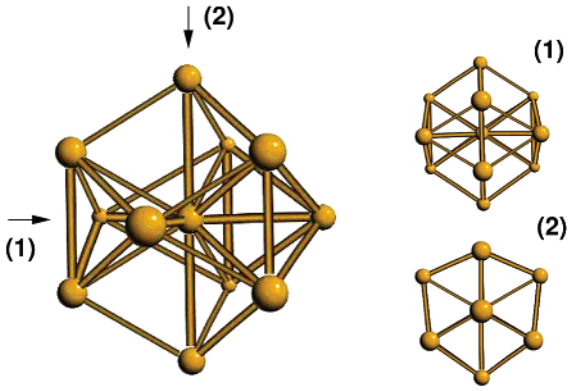

Figure 2. Naked Pt_{12} cluster (on the left side) obtained in an FPMD simulation after the annealing of 12 Pt(0) atoms starting from an arbitrary BCC structure. One of the three 2-fold symmetry axes present in the cluster is labeled with **(1)**, and a 3-fold symmetry axis is labeled with (2). Views along both axes are shown on the right side.

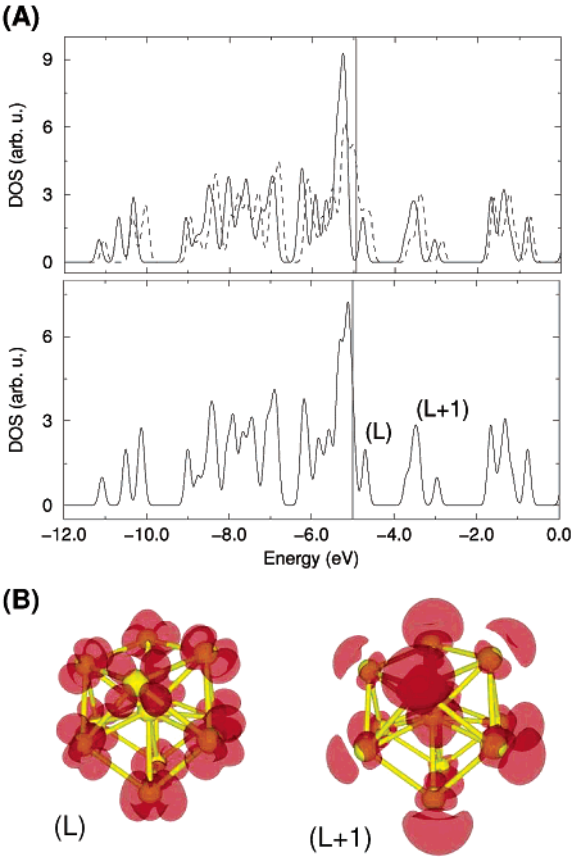

Figure 3. (A) Plot of the density of states (DOS) of a naked Pt_{12} cluster (see Figure 2). Top: spin-unrestricted calculation. (—) Spin-majority component. (- -) Spin-minority component. Bottom: spin-paired calculation. (B) Charge density associated with the LUMO (left) and the LUMO + 1 (right) peaks of the DOSs labeled (L) and (L + 1) in (A).

HOMO−LUMO energy gap is 0.10 eV. Plots of the DOS in the $S = 2$ and $S = 0$ cases are shown in Figure 3 A. In both cases, the characteristic features of the DOS are the LUMO peak (labeled with (L)) and the LUMO + 1 peak (labeled with (L + 1)), separated by a gap of about 1.0 eV. The charge density associated with both peaks in the $S = 0$ case is shown in Figure 3B. The empty orbital lobes of the LUMO + 1 peak protrude widely out of the cluster surface and are thus expected to be highly reactive acceptor sites in addition reactions. In particular, donation into this orbital can be expected to occur from the filled d_{z^2} orbital of square-planar Pt(II) complexes. The reaction of a $PtCl_2(H_2O)_2$ complex with the naked Pt_{12} cluster is studied in the next section by a spin-paired FPMD simulation. Since the DOS near the Fermi level in the spin-paired case is very similar to that found in the spin-polarized case, we can expect to observe in this simulation a cluster reactivity similar to the one that we would observe in a full spin-polarized FMPD simulation. (See also section IIID.)

C. Reaction of $PtCl_2(H_2O)_2$ with a Naked Pt_{12} Cluster. 1. Gas-Phase Simulations. The reaction of the naked Pt_{12} cluster with an unreduced $PtCl_2(H_2O)_2$ complex is studied with a microcanonical FPMD simulation (Figure 4.) During the dynamics, the instantaneous kinetic energy of the system corresponds to a temperature oscillating between 250 and 350 K. In the initial configuration, the Pt−Pt distance between the Pt(II) atom of the complex and the nearest Pt(0) atom of the cluster is about 3.7 Å (Figure 4A). The Pt(II) complex initially approaches the surface of the cluster with the formation of a Pt−Pt bond along the Pt(II) complex's *z* axes. At this point, one of the Cl^- ligands moves toward the underlying cluster and forms a bridge between one atom of the cluster and the Pt(II) atom (Figure 4B). After this, the same ligand detaches from the Pt(II) atom and remains on the cluster surface (Figure 4C). At the same time, one of the water ligands desorbs from the complex and remains free for the rest of the simulation. The Pt atom initially belonging to the Pt(II) complex forms up to three Pt−Pt bonds with atoms of the cluster (Figure 4C), with a mean Pt−Pt distance of 2.76 Å. During the formation of new Pt−Pt bonds, the whole structure of the cluster changes, and an uncapped icosahedral geometry is eventually reached, with the additional atom tightly bound to one of the lateral facets (Figure 4D). After about 5 ps of total simulated time, the atomic motion is quenched to the equilibrium (Figure 4D).

The final structure in Figure 4D does not present a fully compact metallic frame. Indeed, the obtained structure should be assumed to be a local minimum of the potential energy surface in which the system remains trapped during the limited time accessible to the FPMD simulations. To better explore the phase space of the system, we perform a second simulation of the same reaction starting with a different geometry of the Pt_{12} cluster (Figure 5).

The chosen initial structure corresponds to the highest mean coordination number (33 Pt−Pt bonds are present in the cluster) among the Pt_{12} cluster structures considered in ref 24. The reaction proceeds, as in the previous case, with the initial formation of a Pt−Pt bond between the Pt(II) complex and the cluster (Figure 5A and B), followed by the breaking of the complex (Figure 5B and C), whereas the additional Pt atom is fully incorporated into the cluster in less than 3 ps of simulated time (Figure 5C and D). In this case, the local minimum reached at the end of the simulation has a compact structure with 34 Pt−Pt bonds (counting as bound all pairs of atoms located less than 3.0 Å apart from each other). In both simulations, one or two water ligands are observed to detach and move away from the Pt(II) complex during the addition reaction. Furthermore, in the simulation shown in Figure 5, a water molecule binds to the cluster on the opposite side with respect to the initial position of the Pt(II) complex. (This water molecule is actually the repeated image of a former water ligand because of the periodic boundary conditions used.) These observations indicate that the growing cluster's surface interacts rather actively with water ligands, as addressed in the next section.

2. Simulations in a Water Environment. To investigate the effect of the water environment on the addition reaction, we

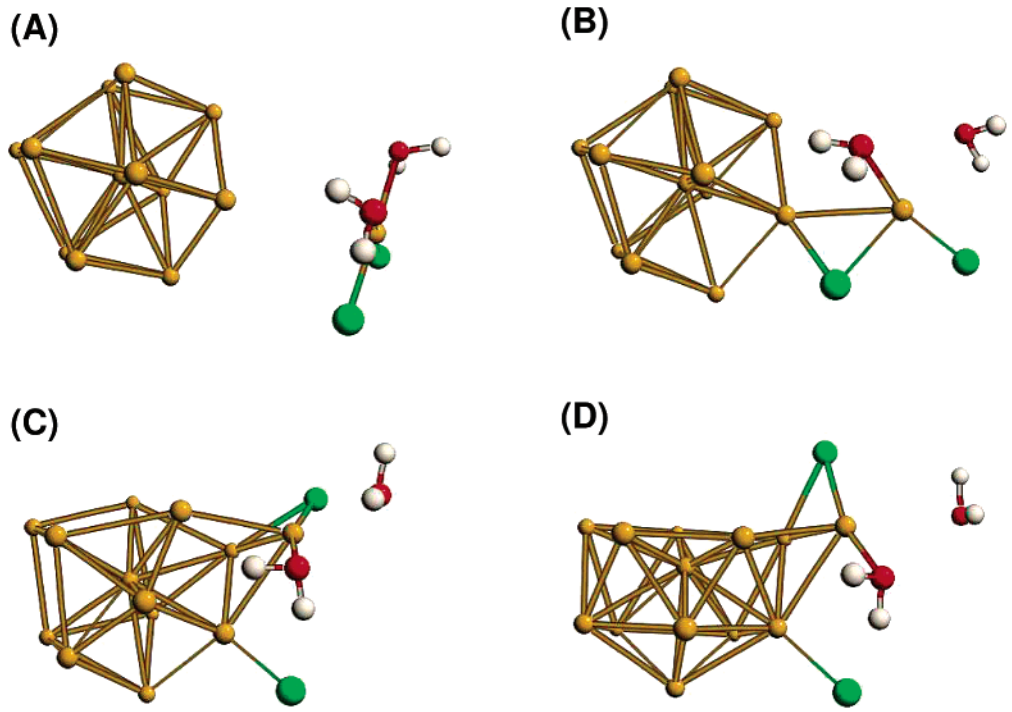

Figure 4. Snapshots from the first FPMD simulation showing the reaction of a $PtCl_2(H_2O)_2$ complex with a naked Pt_{12} cluster. Pt: yellow; Cl: green; O: red; H: white. (A) Initial configuration. (B) After ~0.5 ps of simulated time, the Pt(II) complex adsorbs on the cluster surface with the formation of a direct Pt−Pt bond and a bridge through one of the Cl^- ligands. (C) After about 2 ps, the Pt(II) atom has formed three bonds with atoms of the cluster, leaving the Cl^- ligand on the cluster surface. (D) Final configuration after about 5 ps of simulation time.

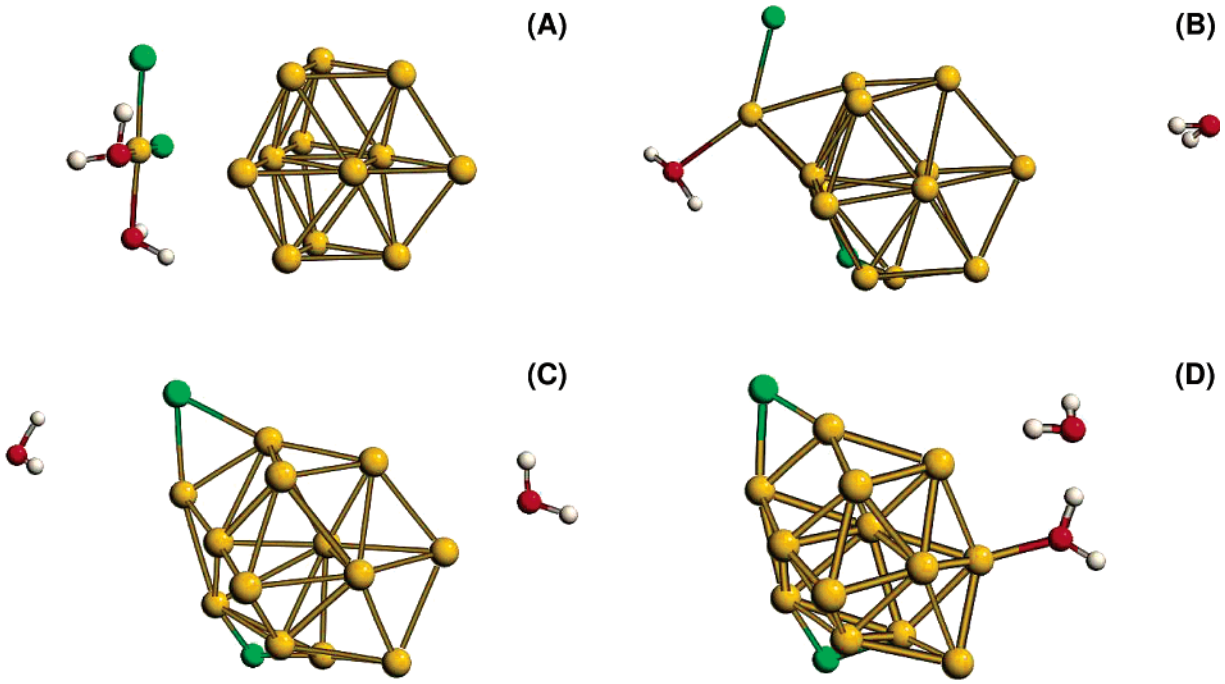

Figure 5. Snapshots from a second FPMD simulation showing the reaction of a $PtCl_2(H_2O)_2$ complex with a naked Pt_{12} cluster having different geometry from the cluster in the previous simulation (Figure 4). Pt: yellow; Cl: green; O: red; H: white. (A) Initial configuration. (B) 1.9 ps of simulation time. (C) 2.8 ps. (D) 3.6 ps.

perform a dynamical simulation of the naked Pt_{12} cluster shown in Figure 2, which is placed in a cubic simulation cell with edge lengths of 13.5 Å. The space surrounding the cluster is this time filled with 53 water molecules (approximately corresponding to the density of bulk water at 300 K). In the initial configuration, 11 of the water molecules are covalently bound to the 11 Pt atoms of the cluster surface, with a Pt−O distance of 2.20 Å, and the remaining 42 water molecules are placed randomly in the cell (Figure 6A). The system is relaxed and gently heated to about 300 K, at which point a microcanonical simulation is started. Fairly soon, we observe one of the water molecules initially bound to the cluster *detaching* from it. Namely, the Pt−O distance increases, becoming larger than 3.0 Å and eventually reaching 3.3 Å (Figure 6B) after about 300 fs, at which point the simulation is stopped. This indicates that water molecules are only weakly bound to Pt clusters in solution and that random fluctuations at room temperature are sufficient to cause a temporary desorption of water ligands from the cluster

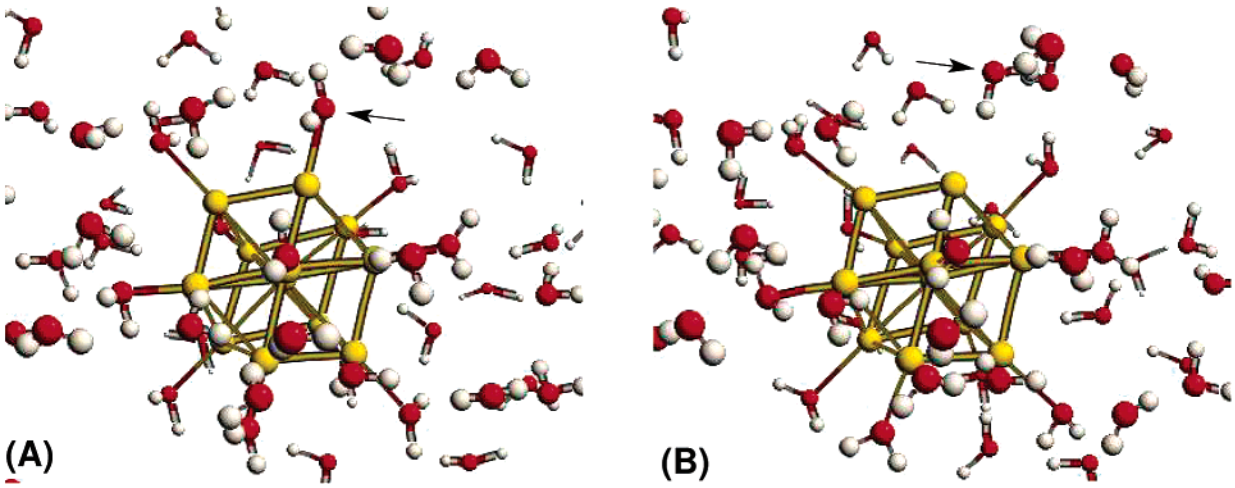

Figure 6. Snapshots from an FPMD simulation of a naked Pt_{12} cluster immersed in water. Pt: yellow; O: red; H: white. (A) Initial configuration. Water molecules (11) are covalently bound to the 11 Pt atoms of the cluster surface (initial Pt−O distance: 2.2 Å), and another 42 molecules are randomly placed in the simulation cell. (B) After about 300 fs of simulated time, one of the water molecules (indicated with a black arrow) has detached from the cluster surface (Pt−O distance: 3.3 Å).

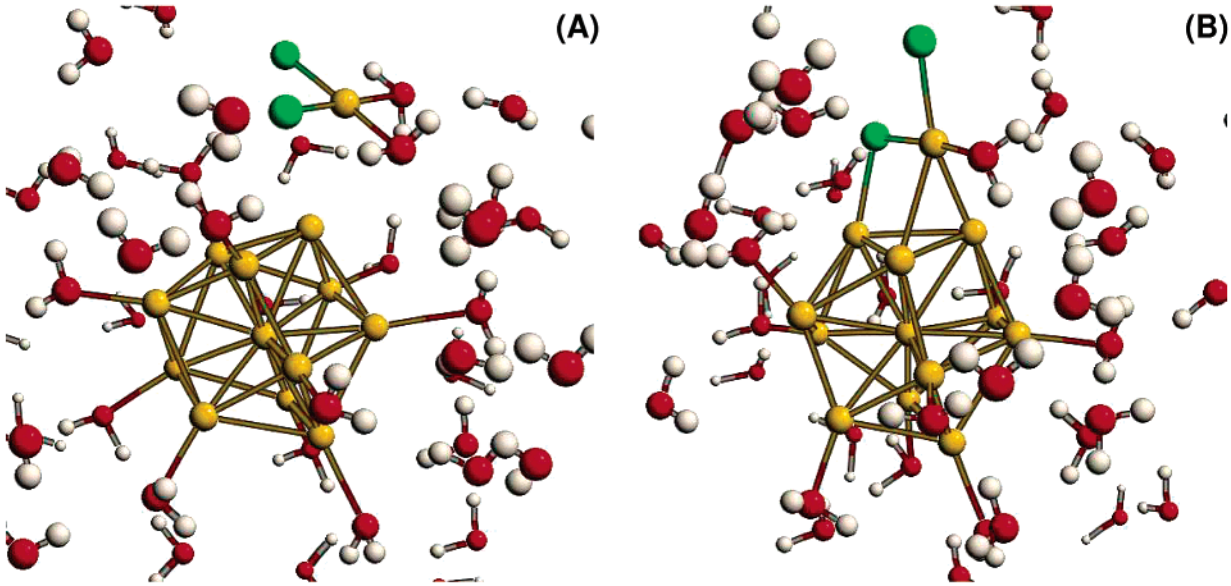

Figure 7. Snapshots from an FPMD simulation showing the reaction of a $PtCl_2(H_2O)_2$ complex with a $Pt_{12}(H_2O)_{10}$ cluster in a simulation cell filled with water molecules. Pt: yellow; Cl: green; O: red; H: white. (A) Initial configuration. (B) 1.5 ps of simulation time.

surface. This exposes metal atoms of the cluster surface to other molecular species present in solution, in particular, allowing for reactions with Pt(II) complexes.

We simulate the reaction between Pt(II) complexes and metallic Pt clusters immersed in water in a constant-temperature FPMD simulation at 300 K, starting with a $PtCl_2(H_2O)_2$ complex positioned near the $Pt_{12}(H_2O)_{10}$ cluster obtained at the end of the previous simulation (Figure 7). This system is placed in a $15 \times 13 \times 13$ Å^3 cell filled with 36 additional water molecules, setting the initial distance between the Pt(II) atom and the nearest Pt atom of the cluster equal to 3.23 Å (Figure 7A). The addition reaction is once more observed. It proceeds exactly as observed in the gas-phase simulations, with the initial formation of a Pt−Pt bond along the *z* axes of the Pt(II) complex, followed by the detachment of one of the water ligands from the Pt(II) atom. The reaction continues with the formation of a second Pt−Pt bond between the complex and the cluster, and after about 1.5 ps of simulated time, one of the chlorine ligands binds to the cluster surface (Figure 7B). As a consequence of the addition process, two of the adsorbed water molecules detach from the cluster surface.

D. Reaction of $PtCl_2(H_2O)_2$ with a $Pt_{12}Cl_4$ Cluster. In the previous simulations, we observed the reactions between unreduced Pt(II) complexes and fully reduced Pt_{12} clusters. However, according to the mechanism of cluster formation earlier proposed in ref 1, the reduction to the zero-valent state is not a necessary condition for cluster growth. In particular, under mild reducing conditions, the addition of complexes to a growing cluster can be expected to occur before the complete reduction of the cluster to the metallic state. With the aim of simulating the process of cluster growth under mild reducing conditions, we now consider the addition of Pt(II) complexes to partially oxidized clusters. For this, we increase the global oxidation state of the Pt_{12} cluster shown in Figure 2 by adding four chlorine ligands on its surface, keeping the whole system neutral. Full relaxation of the $Pt_{12}Cl_4$ structure leads to a minimum-energy configuration where the metal core atomic structure is not altered by the addition of the chlorine ligands. The equilibrium Pt−Cl distances are all equal to 2.24 Å. The relaxed structure is shown in Figure 8 together with the empty orbital states above the Fermi level, which are mainly localized on the Pt atoms free of ligands (cf. Figure 3 bottom right). As

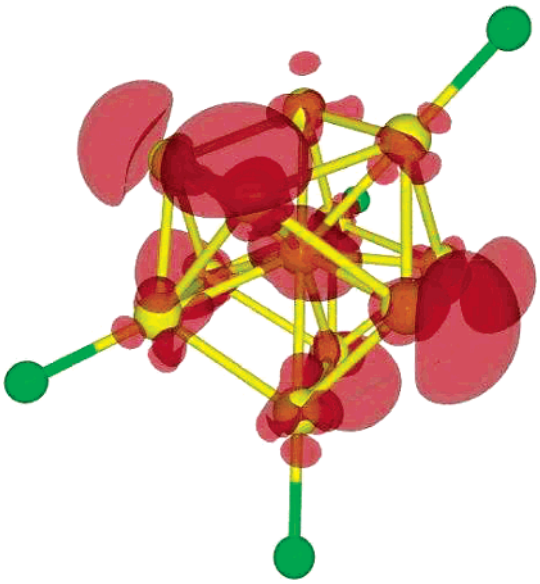

Figure 8. Relaxed structure of the $Pt_{12}Cl_4$ cluster considered in the simulations. (See the text, section IIID.) The empty states above the Fermi level are depicted with a red semitransparent isosurface.

in the case of the naked Pt_{12} cluster, these empty orbital lobes are expected to act as acceptors of electrons from closed shells of Pt(II) complexes during aggregation reactions. The reaction of $Pt_{12}Cl_4$ with a $PtCl_2(H_2O)_2$ complex is investigated with a microcanonical FPMD simulation, where the temperature oscillates around 300 K and is never higher than about 350 K (Figure 9). The initial distance between the Pt(II) atom and the nearest Pt atom of the cluster is set to ∼3.7 Å (Figure 9A). Once more, the $PtCl_2(H_2O)_2$ complex is soon adsorbed on the cluster surface (Figure 9B), forming a Pt−Pt bond along the *z* axis of the square-planar complex. Later, the chlorine ligands also bind to Pt atoms of the cluster (Figure 9B and C). As in the previous simulations, the Pt(II) atom starts forming several bonds with the other Pt atoms. After about 2 ps of simulated time, the Pt atom originally belonging to the Pt(II) complex is completely incorporated into the cluster structure, which consists at this point of a central Pt atom coordinating the other 12 Pt atoms surrounding it (Figure 9D). Six chlorine ligands are adsorbed on the cluster surface. Remarkably, despite the magic number nuclearity of the formed cluster (Pt_{13} is the first atomic closed shell[42,43]), this spheroidal structure is *not* a local minimum of the potential energy surface. Indeed, by continuing the simulation, we observe the central atom moving off of its position (Figure 9E). The cluster completely rearranges itself at this point, and a structure consisting of three stacked slabs of Pt atoms disposed in a triangular lattice is obtained after ∼3.2 ps of simulated time. The system remains in this configuration for ∼1.8 ps more, after which the atomic motion is slowly quenched. The final equilibrium structure is shown in Figure 9F.

As a check of the validity of the spin-paired approximation in the systems considered, we perform a new FPMD simulation starting from the same initial conditions of Figure 9A but treat the occupation numbers of the up and down spin components as independent variables and lower the smearing temperature to $k_BT_S = 0.05$ eV. Once again, the Pt(II) complex soon adsorbs on the cluster, whereas one of the chlorine ligands is detached from the Pt(II) atom and is left on the cluster surface. After the formation of three Pt−Pt bonds between the Pt(II) atoms and the cluster, this simulation was stopped.

The evolution of the DOS of the system during the reaction observed in the spin-paired simulation is illustrated in Figure 10. It is particularly interesting to follow the evolution of the $d_{x^2-y^2}$ LUMO state of the $PtCl_2(H_2O)_2$ complex during the reaction with the $Pt_{12}Cl_4$ cluster. At the beginning of the simulation, this state is localized on the Pt(II) complex (Figure 10 bottom, snapshot (1)), and its associated energy level is located just above the gap separating the d electronic shell of the cluster from the higher levels (Figure 10 top, curve (1)). Immediately after the formation of a Pt−Pt bond between the Pt(II) atom and one of the Pt atoms of the cluster, the same state becomes delocalized over the whole cluster (Figure 10 bottom, snapshot (2)). The corresponding energy level is lowered by about 0.6 eV and reaches the upper edge of the cluster's d electronic shell (Figure 10 top, curve (2)). At the end of the simulation, the position in energy of this state is nearly the same (Figure 10 top, curve (3)), whereas the electron delocalization is even more evident (Figure 10 bottom, snapshot (3)), and the atom initially belonging to the Pt(II) complex is thus completely indistinguishable from the other atoms composing the cluster.

E. Reaction of $PtCl_2(H_2O)_2$ with a $Pt_{13}Cl_6$ Cluster. We performed one more FPMD simulation to model a further addition step of Pt(II) complexes to a growing cluster in a high oxidation state. A $PtCl_2(H_2O)_2$ complex is initially placed near the optimized cluster structure $Pt_{13}Cl_6$ that was obtained in the previous simulation (Figure 11A). The distance between the Pt(II) atom and the nearest Pt atom of the cluster is set equal to ∼3.6 Å. Once again, the Pt(II) complex is soon adsorbed on the cluster surface, and at the end of the simulation, the Pt(II) atom is fully incorporated into the cluster structure (Figure 11B−D). The addition reaction proceeds, as in the two precedent cases, with a detachment of ligands from the Pt(II) atom and chlorine adsorption on the cluster surface. This process promotes a rearrangement of the Cl^- ligand distribution. Namely, three chlorine ligands are observed to move in a coordinated way from "on top" positions (Figure 11B) to "bridge" positions (Figure 11C) with respect to the underlying Pt atoms. Later, one of these ligands moves again to an "on top" position on a Pt atom nearby (Figure 11D). This FPMD simulation is stopped after about 5 ps of simulated time. The final structure is shown in Figure 11D.

IV. Discussion

Consistent with the model of cluster nucleation proposed in ref 1, we take into account a mechanism of growth where (i) metal−metal bonds can form between Pt atoms in oxidation states higher than zero and (ii) chlorine ligands remain bound to the Pt atoms during cluster formation and are able to leave the cluster upon reduction. The growth of noble-metal clusters is known to occur through an autocatalytic process where the presence of already-formed clusters facilitates the further steps of reduction and aggregation of new atoms.[5] The reduction of metal complexes is thought to take place in situ on the cluster surface upon the adsorption of unreduced ions.[3,17] In agreement with this experimental observations, our assumption is that Pt(II) complexes react before reduction with a growing cluster present in solution.

A. Cluster Growth via the Addition of Unreduced Pt(II) Complexes. The analysis of the calculated densities of electronic states reveals that naked Pt_{13} and Pt_{12} clusters present an open electronic shell (associated with a ground state of nonzero spin). This is in agreement with other spin-polarized studies of the electronic structure of Pt_{13} clusters.[46−48] The empty states above the Fermi level of the Pt_{12} and $Pt_{12}Cl_4$ clusters considered in

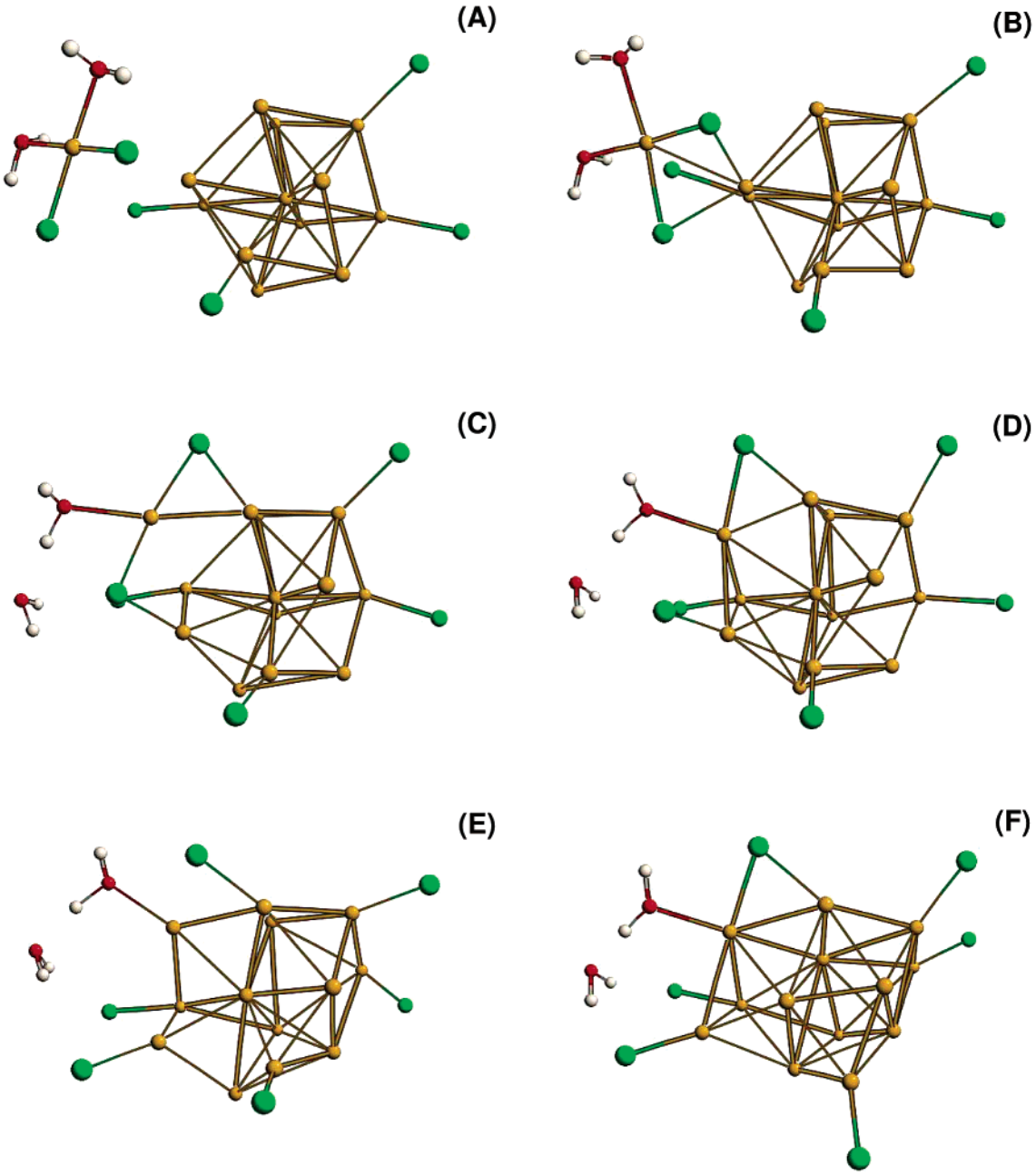

Figure 9. Snapshots from an FPMD simulation showing the reaction of a $PtCl_2(H_2O)_2$ complex with a $Pt_{12}Cl_4$ cluster. (See the text, section IIID.) Pt: yellow; Cl: green; O: red; H: white. (A) 0.0 ps of simulation time. (B) 0.6 ps. (C) 1.3 ps. (D) 2.0 ps. (E) 3.2 ps. (F) 5.0 ps.

our study (Figures 3 and 8) are localized widely outside the cluster surface. This suggests that a reaction between a $PtCl_2$-$(H_2O)_2$ complex and a small cluster can take place via electron donation from the filled d_{z^2} orbital of the Pt(II) complex to the empty orbitals of the clusters. We observe this reaction to occur at room temperature without appreciable energy barriers in a series of FPMD simulations (Figures 4, 5, 7, 9, and 11) both in the gas phase and in simulation cells filled with water molecules to model the solution environment. Taking explicitly into account the water solvent, we observe that water molecules appear to be weakly bound to the surface of metallic clusters and can spontaneously desorb as a consequence of random fluctuations at room temperature (Figure 6). Although a read-sorption of water at a later stage cannot be excluded, this process makes the naked surface of the cluster "visible" for a while to other molecular species, in particular, to Pt(II) complexes, allowing for the observed addition reactions. After the adsorption of a Pt(II) complex on the cluster surface, the reaction proceeds with the immediate breaking of the bonds between the Pt(II) atoms and its ligands and ends with the full incorporation of the Pt(II) atoms into the cluster. The same reaction is observed considering both a fully reduced Pt_{12} cluster (naked or immersed in water) and partially oxidized (and ligated) $Pt_{12}Cl_4$ and $Pt_{13}Cl_6$ clusters.

The analysis of the DOS of the system during the aggregation reveals that the electronic states of the Pt(II) complex become delocalized over the whole cluster structure immediately after the formation of the first Pt−Pt bond (see Figure 10). After the adsorption on the cluster, the additional atom immediately becomes indistinguishable from the other Pt atoms without being trapped in precursor-state geometries. The cluster appears to optimize its cohesive energy by increasing the mean coordination number of *all* of its atoms.[24,27,29] This is achieved by forming several Pt−Pt bonds between the Pt atom originally belonging to the Pt(II) complex and the original Pt cluster atoms, with considerable rearrangements of the whole cluster skeleton

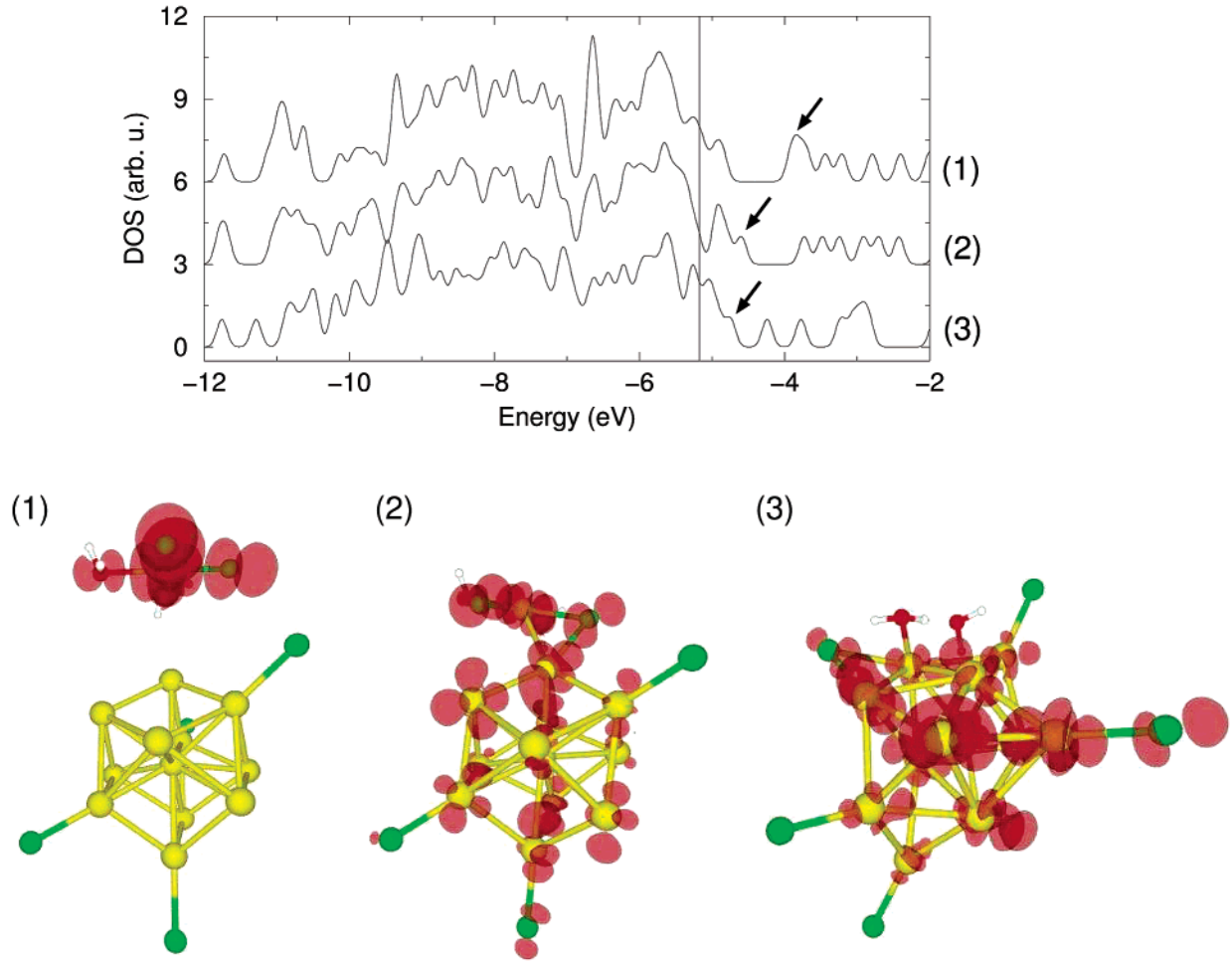

Figure 10. Evolution of the density of state (DOS) of the whole system during the reaction of a $PtCl_2(H_2O)_2$ complex with a $Pt_{12}Cl_4$ cluster. (See the text and Figure 9.) The vertical line indicates the Fermi level. The LUMO state of the Pt(II) complex is depicted in the snapshot (1) (bottom) with a red semitransparent isosurface, and its associated energy level is indicated with an arrow in the corresponding plot of the DOS (curve (1)). Immediately after the formation of the first Pt−Pt bond between the Pt(II) complex and the cluster, this state becomes delocalized over the whole cluster (snapshots (2) and (3)). The corresponding energy level is lowered by about 0.6 eV and reaches the upper edge of the cluster's d electronic shell (curves (2) and (3); see arrow).

being observed in all of our simulations. (See the next section.) This process proceeds until the new atom is fully incorporated into the cluster structure (Figures 5 and 9) and the cluster reaches a (local) minimum of the potential energy surface whose structure bears no obvious "memory" of the incorporation event.

B. Low-Energy Skeleton Rearrangements. In previous investigations, the growth of noble-metal clusters has been studied by considering the structure and energetics of naked clusters with increasing nuclearity.[24−28] Taking into account the reaction $Pt_{n-1} + Pt \rightarrow Pt_n$ (which is expected to be exothermic for all nuclearities n[24]), no obvious pattern appears for the metallic growth. We note that this is consistent with the existence of low- or no energy barriers for the reorganization of the cluster structure after aggregation,[24,25] which can be inferred by all of our dynamical simulations. Namely, we find that for metal clusters of small exposed surface, where the growth kinetics could in principle be slowed by the steric constraints associated with precursor adsorption states, there are low-barrier or barrierless reaction paths for the *direct* incorporation of adsorbates. Indeed, the whole adsorption/rearrangement process is accomplished in a few picoseconds so that the structure is immediately ready for novel adsorption processes. This suggests a nucleation-limited model where the initial dimer formation[1] can be assumed to be the limiting kinetic step of cluster growth. Consistent with this, we note that some mechanism allowing for the efficient accretion of small metal clusters is necessary to rationalize the experimental finding that a biomolecular substrate ligand capable of catalyzing the dimerization step can be used to achieve selectively heterogeneous metallization upon reduction in a metal salt solution.[13]

Our results support a face-capping model of growth[25] leading after every aggregation step to relatively compact cluster structures composed of stacks of atomic layers and associated with high coordination numbers of all of the metal atoms within the cluster.[24] This is consistent with a surface-growth mechanism that was proposed to account for shape-controlled cluster formation.[4] Indeed, the aggregation of complexes into a growing cluster can be selectively limited by the capping action of ligands adsorbed on the cluster surface. In addition, our simulations suggest that easily accessible pathways for structural rearrangement (which are related to the concept of cluster isomerism) and the fluxionality of ligands promoted by condensation reactions[22,51,52] may have to be taken into account to rationalize a specific growth pattern.

C. Effect of the Ligands. It is known that ligands play an important role in stabilizing small metal clusters. Our simulations suggest that the presence of water and chlorine ligands at low concentration is not sufficient to "freeze" the growing metal cores into a stable geometry. In particular, the $Pt_{13}Cl_6$ cluster obtained in one of the simulations (Figure 9) does not present

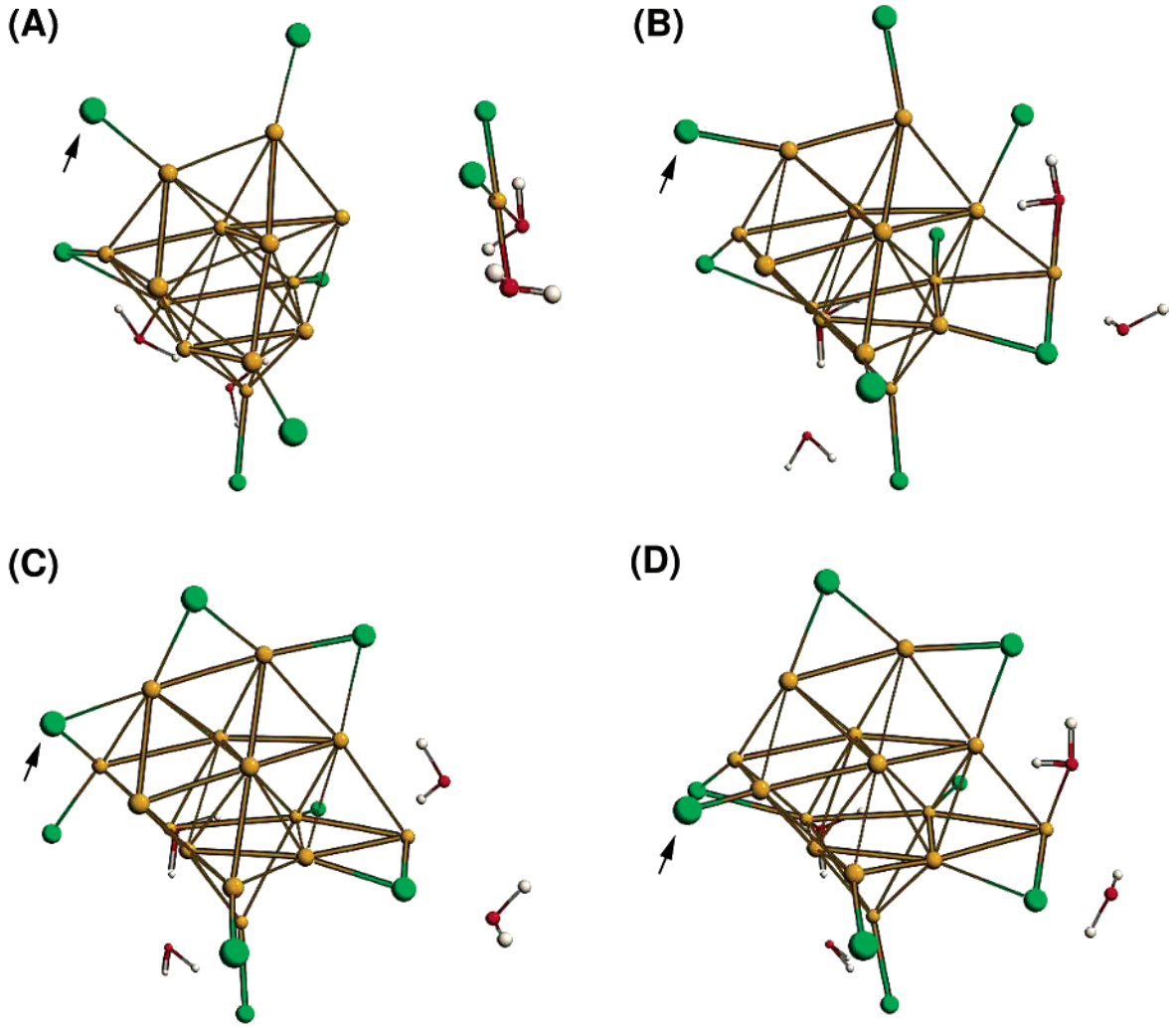

Figure 11. Snapshots from an FPMD simulation showing the reaction of a $PtCl_2(H_2O)_2$ complex with a $Pt_{13}Cl_6$ cluster. Pt: yellow; Cl: green; O: red; H: white. (A) 0.0 ps of simulated time. (B) 1.4 ps. (C) 3.5 ps. (D) 5.2 ps. The arrow indicates a chlorine ligand that changes adsorption sites during the simulation.

a closed-shell geometry of the metal atoms (i.e., icosahedral or cubooctahedral), as observed in the case of strongly ligated M_{13} clusters.[22] On the contrary, a geometry where a central Pt atom is surrounded by the other atoms is reached during an FPMD simulation (Figure 9D) but is *not* a minimum of the potential energy surface. Namely, in the spontaneous evolution of the system, the central atom moves off of its position, and a structure consisting of three stacked layers of atoms arranged in a triangular lattice is eventually obtained. This open geometry of the cluster offers further reactive sites for the addition of unreduced complexes, as we observed in a successive simulation (Figure 11). Therefore, in the absence of strong capping agents, a growth process involving mild reducing agents is not expected to stop after the formation of small clusters. This is consistent with the fact that the cluster size distributions obtained after the reduction of dissolved K_2PtCl_4 in the presence of surfactants weakly bound to the cluster surface are normally centered on much larger nuclearities.[53] Small magic-number clusters consisting of 13 or 55 noble-metal atoms are indeed stabilized only by complex ligand systems.[54]

D. Autocatalytic Surface-Growth Mechanism. From the kinetics of the formation of noble-metal clusters, an autocatalytic surface-growth mechanism has been inferred[5,7] where the metal complexes are reduced in situ on the surface of a growing cluster. In our simulations, we observe that the aggregation of Pt(II) to small clusters occurs spontaneously without the need of additional reducing electrons even if the clusters are not completely reduced to the metallic state. The reduction process may thus take place at a later stage involving the whole formed cluster and not the isolated complexes. We note that if in the presence of weak stabilizers the aggregation reaction occurs without difficulties (in our simulations it takes place spontaneously at room temperature) then the whole process of cluster formation can be limited only by the rate of electron transfer between the reducing agent and the growing cluster. However, since the growth proceeds via the addition of unreduced complexes, the global oxidation state of the cluster increases when the cluster nuclearity changes, with the effect of enhancing the affinity of the cluster for reducing electrons and thus facilitating the electron transfer. This appears to be consistent with the observed autoaccelerated kinetics of the process of cluster growth.[5] We finally note that the addition of unreduced complexes to partially reduced units (atoms or clusters) takes place from the very beginning of the reduction/growth process.[1] In other words, the molecular mechanisms leading to the nucleation (dimer formation) and growth of platinum clusters appear to be the same. However, the nucleation stage can still be resolved from the subsequent growth stage if the kinetics of the reduction of an isolated complex is much slower than the reduction kinetics of the first formed clusters. In particular, in

experiments using relatively weak reducing agents, the precipitation of metal can be selectively promoted by the presence of nucleation seeds such as, for example, preformed metal clusters[18] or a number of metal complexes that are easy to reduce.[13] On the contrary, in the presence of sufficiently strong reducing agents, any reduced complex species will provide a "critical" nucleus for stable cluster growth.

V. Summary

The molecular mechanism of cluster growth upon the reduction of hydrolyzed $PtCl_4^{2-}$ ions is studied in a series of FPMD simulations. We consider a model of growth where unreduced $PtCl_2(H_2O)_2$ complexes react with neutral clusters before reduction. Both in gas-phase simulations and in simulations that explicitly take into account the water environment we observe that the Pt(II) complexes can spontaneously react with Pt_{12}, $Pt_{12}Cl_4$, and $Pt_{13}Cl_6$ clusters and are completely incorporated into the cluster structure. The aggregation takes place with a considerable rearrangement of the cluster structure and involves a redistribution of the chlorine ligands on the cluster surface. The adsorption reaction is promoted by electron donation from the filled d_{z^2} orbital of the square-planar Pt(II) complexes to the empty orbitals of the open-shell clusters that extend outside the cluster surface. This is followed by the full incorporation of the Pt atom originally belonging to the Pt(II) complex into the cluster structure, which increases the mean atomic coordination number and thus the cohesive energy per atom of the whole cluster. The energy barriers associated with the adsorption/incorporation process appear to be negligible at room temperature, suggesting that, in general, low-energy structural rearrangements and ligand fluxionality should be taken into account to realize a controlled growth of noble-metal clusters in reduction baths. The mechanism suggested by the simulations is fully consistent with the autoaccelerating kinetics of the process of cluster growth and with a face-capping growth mechanism that can account for shape-controlled cluster fabrication.

Acknowledgment. M. Mertig is kindly acknowledged for fruitful discussions. We thank M. Stengel for his continuous and precious help on all kinds of technical issues. CPU time allocation has been provided by the Center for High Performance Computing of the Dresden University of Technology. L.C.C. and A.D.V. acknowledge support from the IRRMA institute in Lausanne.

Note Added after ASAP Posting. This article was posted ASAP on 2/4/2003 and reposted on 2/7/2003 with additional information in the contribution line for Alessandro De Vita.

References and Notes

(1) Colombi Ciacchi, L.; Pompe, W.; De Vita, A. *J. Am. Chem. Soc.* **2001**, *123*, 7371.

(2) Henglein, A.; Giersig, M. *J. Phys. Chem. B* **2000**, *104*, 6767.

(3) Belloni, J.; Mostafavi, M. In *Metal Clusters in Chemistry*; Braunstein, P., Oro, L. A., Raithby, P. R., Eds; Wiley-VHC: New York, 1999; pp 1213−1247.

(4) Petroski, J. M.; Wang, Z. L.; Green, T. C.; El-Sayed, M. A. *J. Phys. Chem. B* **1998**, *102*, 3316.

(5) Watzky, M. A.; Finke, R. G. *J. Am. Chem. Soc.* **1997**, *119*, 10382.

(6) Pan, C.; Pelzer, K.; Philippot, K.; Chaudret, B.; Dassenoy, F.; Lecante, P.; Casanove, M.-J. *J. Am. Chem. Soc.* **2001**, *123*, 7584.

(7) Aiken, J. D., III.; Finke, R. G. *J. Am. Chem. Soc.* **1998**, *120*, 9545.

(8) Ahmadi, T. S.; Wang, Z. L.; Green, T. C.; Henglein, A.; El-Sayed, M. A. *Science (Washington, D.C.)* **1996**, *272*, 1924.

(9) Clint, J. H.; Collins, I. R.; Williams, J. A.; Robinson, B. H.; Towey, T. F.; Cajean, P.; Kahn-Lodhi, A. *Faraday Discuss. Chem. Soc.* **1993**, *95*, 219.

(10) Schmid, G.; Bäumle, M.; Beyer, N. *Angew. Chem.* **2000**, *112*, 187−189. Schmid, G.; Bäumle, M.; Beyer, N. *Angew. Chem., Int. Ed.* **2000**, *39*, 181.

(11) Shipway, A. N.; Katz, E.; Willner, I. *ChemPhysChem* **2000**, *1*, 18.

(12) Li, J.-L.; Jia, J.-F.; Liang, X.-J.; Liu, X.; Wang, J.-Z.; Xue, Q.-K.; Li, Z.-Q.; Tse, J. S.; Zhang, Z.; Zhang, S. B. *Phys. Rev. Lett.* **2002**, *88*, 066101.

(13) Mertig, M.; Colombi Ciacchi, L.; Seidel, R.; Pompe, W.; De Vita, A. *Nano Lett.* **2002**, *2*, 841.

(14) Payne, M. C.; Teter, M. P.; Allan, D. C.; Arias, T. A.; Joannopoulos, J. D. *Rev. Mod. Phys.* **1992**, *64*, 1045.

(15) Car, R.; Parrinello, M. *Phys. Rev. Lett.* **1985**, *55*, 2471.

(16) Furlong, D. N.; Launikonis, A.; Sasse, W. H. F.; Sanders, J. V. *J. Chem. Soc., Faraday Trans. 1* **1984**, *80*, 571.

(17) Henglein, A.; Meisel, D. *Langmuir* **1998**, *14*, 7392.

(18) Henglein, A. *Langmuir* **2001**, *17*, 2329.

(19) Henglein, A. *J. Phys. Chem. B* **2000**, *104*, 1206.

(20) Leff, D. V.; Ohara, P. C.; Heath, J. R.; Gelbart, W. M. *J. Phys. Chem.* **1995**, *99*, 7036.

(21) Whetten, R. L.; Gelbart, W. M. *J. Phys. Chem.* **1994**, *98*, 3544.

(22) Allevi, C.; Heaton, B. T.; Seregni, C.; Strona, L.; Goodfellow, R. J.; Chini, P.; Martinengo, S. *J. Chem. Soc., Dalton Trans.* **1986**, 1375.

(23) Mafuné, F.; Kohno, J.-y.; Takeda, Y.; Kondow, T. *J. Phys. Chem. B* **2002**, *106*, 8555.

(24) Bigot, B.; Minot, C. *J. Am. Chem. Soc.* **1984**, *106*, 6601.

(25) Wales, D. J.; Kirkland, A. I.; Jefferson, D. A. *J. Chem. Phys.* **1989**, *91*, 603.

(26) Yang, S. H.; Drabold, D. A.; Adams, J. B.; Ordejón, P.; Glassford, K. *J. Phys.: Condens. Matter* **1997**, *9*, L39.

(27) Rösch, N.; Ackermann, L.; Pacchioni, G. *Chem. Phys. Lett.* **1992**, *199*, 275.

(28) Jennison, D. R.; Schultz, P. A.; Sears, M. P. *J. Chem. Phys.* **1997**, *106*, 1856.

(29) Häberlen, O. D.; Chung, S.-C.; Stener, M.; Rösch, N. *J. Chem. Phys.* **1997**, *106*, 5189.

(30) Gunnarsson, O.; Lundqvist, B. I. *Phys. Rev. B* **1976**, *13*, 4274.

(31) Perdew, J. P.; Wang, Y. *Phys. Rev. B* **1992**, *45*, 13244.

(32) Troullier, N.; Martins, J. L. *Phys. Rev. B* **1991**, *43*, 1993.

(33) Pacchioni, G.; Rösch, N. In *Metal Clusters in Chemistry*; Braunstein, P., Oro, L. A., Raithby, P. R., Eds.; Wiley-VHC: New York, 1999; pp 1393−1433.

(34) Ballone, P.; Andreoni, W. In *Metal Clusters*; Ekardt, W., Ed.; Wiley: New York, 1999; pp 71−144.

(35) Vande Vondele, J.; De Vita, A. *Phys. Rev. B* **1999**, *60*, 13241.

(36) Stengel, M.; De Vita, A. *Phys. Rev. B* **2000**, *62*, 15283.

(37) As a check, one of the dynamical simulations has been performed with smearing energies of 0.25 and 0.05 eV. No qualitative differences in the simulated trajectory have been observed. (See section IIID.)

(38) The bulk properties of Pt are computed using 60 **k** points in the irreducible wedge of the Brillouin zone and expanding the Bloch functions up to a kinetic energy cutoff of 70 Ry.

(39) Olsen, R. A.; Kroes, G. J.; Baerends, E. J. *J. Chem. Phys.* **1999**, *111*, 11155.

(40) Kittel, C. *Introduction to Solid-State Physics*, 6th ed.; Wiley: New York, 1986.

(41) De Vita, A.; Canning, A.; Car, R. *EPFL Supercompt. J.* **1994**, *6*, 22.

(42) Chini, P. *Gazz. Chim. Ital.* **1979**, *109*, 225. Chini, P. *Organomet. Chem.* **1980**, *200*, 37.

(43) Mackay, A. L. *Acta Crystallogr.* **1962**, *15*, 916.

(44) Schmid, G.; Klein, N.; Morun, B.; Lehnert, A. *Pure Appl. Chem.* **1990**, *62*, 1175.

(45) In a recent spin-polarized DFT calculation of naked clusters,[46] the icosahedral geometry was found to be more stable than the cubooctahedral geometry both for Pt_{13} and for Pd_{13} clusters. Other authors found instead that the icosahedral geometry is the most stable for Pd_{13} clusters,[49,50] and that amorphous structures are the ground state for Pt_{13} clusters. (See ref 26 and references therein.) These differences are mainly due to the different techniques used in the theoretical calculations and are not relevant for the scope of this work.

(46) Watari, N.; Ohnishi, S. *Phys. Rev. B* **1998**, *58*, 1665.

(47) Watari, N.; Ohnishi, S. *J. Chem. Phys.* **1997**, *106*, 7531.

(48) Aprà, E.; Fortunelli, A. *THEOCHEM* **2000**, *501−502*, 251.

(49) Reddy, B. V.; Khanna, S. N.; Dunlap, B. I. *Phys. Rev. Lett.* **1993**, *70*, 3323.

(50) Estiú, G. L.; Zerner, M. C. *J. Phys. Chem.* **1994**, *98*, 4793.

(51) Lawson, R. J.; Shapely, J. R. *J. Am. Chem. Soc.* **1976**, *98*, 7433.

(52) Farrugia, L. J.; Orpen, A. G. In *Metal Clusters in Chemistry*; Braunstein, P., Oro, L. A., Raithby, P. R., Eds.; Wiley-VHC: New York, 1999; pp 1001−1027.

(53) Van Rheenen, P. R.; McKelvy, M. J.; Glausinger, W. S. *J. Solid State Chem.* **1987**, *67*, 151.

(54) Schmid, G.; Pugin, R.; Malm, J.-O.; Bovin, J.-O. *Eur. J. Inorg. Chem.* **1998**, 813.